Tests of two time-dependent seismicity models based on interevent times of mainshocks and on seismic triggering in the Aegean area

B.C. Papazachos, G.F. Karakaisis, C.B. Papazachos and E.M. Scordilis

Department of Geophysics, Thessaloniki, Greece

(Received: June 8, 2010; accepted: November 27, 2010)

ABSTRACT In the present work, the basic principles and recent developments of two intermediate-term prediction models are described. The first one is the Time and Magnitude Predictable regional model which is based on interevent times of strong (M>6.0) mainshocks while the second one is the Decelerating-Accelerating Strain model which is based on the triggering of a mainshock by its preshocks. A combined forward test of both these models is performed by attempting estimation (prediction) of probably ensuing strong mainshocks in the broader Aegean area (Aegean Sea and surrounding lands). The results led to the identification of six regions that are candidates for the generation of strong (M>6.0) mainshocks during the next eight years (2010-2017). The uncertainties in the estimation of the parameters of these six probably ensuing mainshocks are: ±2.5 years in the origin time, ≤120 km in the epicenter, h≤100 km in the focal depth and ±0.3 in the magnitude, with an about 80% probability.

1. Introduction

Despite over a century of research efforts, the ideal target for the seismologist's short term earthquake prediction remains a very difficult to reach and, for this reason, is still an unsolved scientific problem. However, research work during recent decades raises hopes for intermediate term prediction on the basis of interevent times of strong mainshocks, as well as the triggering of strong earthquakes by their preshocks. Currently available interevent times of large earthquakes (Fedotov, 1965; Shimazaki and Nakata, 1980) are the seismological data (historical, instrumental) that can be useful to improve our knowledge of intermediate term earthquake prediction. Unfortunately, there is a limited number of strong earthquakes that have occurred on a seismic fault for which relatively reliable information (size, origin time) is available for robust statistical analysis. For this reason, and since neighboring faults interact, "networks of neighboring seismic faults" have been considered as target groups for intermediate-term prediction. On the basis of this idea, the Time and Magnitude Predictable (TIMAP) regional model has been formulated (Papazachos *et al*., 1997). By examining groups of faults, this model treats a large sample of interevent times of strong earthquakes generated in a region for a reliable study of time dependent seismicity. Recently, the model has been further developed by backward tests in the Aegean area (Papazachos *et al*., 2010b).

Another approach has been the Decelerating-Accelerating Strain (D-AS) model for intermediate term prediction of strong mainshocks. This is based upon the assumption that fluctuation of tectonic stress is expressed by corresponding deviation of seismicity from the

background. Such seismicity deviations can be positive (seismic excitations) or negative (seismic quiescence) and several precursory seismicity patterns based on such deviations have been proposed for improving knowledge on intermediate term earthquake prediction.

The main goal of the present work is to perform forward tests of both TIMAP and D-AS models by using the seismological data for the broader Aegean area (34^0N-43^0N, 19^0E-30^0E) available up to September 30, 2009 and to attempt a forward estimation (prediction) of probable ensuing strong mainshocks during the next years. Such a forward test of the D-AS model has been already presented (Papazachos *et al*., 2009) but the present test concerns the combined application of both TIMAP and D-AS models. The new test also incorporates additional new data for two recent years (2008, 2009). Thus, the combined application of the two models and the new additional data helped to improve previous estimations (predictions) and to identify additional regions which exhibit properties of precursory seismicity.

2. The Time and Magnitude Predictable (TIMAP) Model

Papazachos *et al*. (1997) used a very large sample of global data to define the relations:

$$\log T_t = 0.19 M_{\min} + 0.33 M_p + Q \tag{1}$$

$$M_f = 0.73 M_{\min} - 0.28 M_p + W \tag{2}$$

where T_t (in years) is the interevent time, M_{min} is the minimum mainshock magnitude considered, M_p is the magnitude of the previous mainshock in the seismic region and M_f is the magnitude of the following mainshock in the region. Q and W are constants that depend on the long-term seismicity level of the seismic region and their mean values and the corresponding standard deviation σ_q and σ_w are calculated by the available data for each region.

It has been also shown (Papazachos and Papaioannou, 1993; Papazachos *et al*., 1997) that the ratio T/T_t of the observed interevent time, T, to the calculated, T_t, by Eq. (1) follows a lognormal distribution with a mean equal to zero and a standard deviation, σ. This behavior allows the calculation of the probability, P, for the occurrence of a mainshock with $M>M_{min}$ during the next Δt years, if the previous such mainshock ($M_p>M_{min}$) occurred t years ago, using the relation:

$$P(\Delta t) = \frac{F\left(L_2/\sigma\right) - F\left(L_1/\sigma\right)}{1 - F\left(L_1/\sigma\right)} \tag{3}$$

where $L_2 = \log\frac{t+\Delta t}{T_t}$, $L_1 = \log\frac{t}{T_t}$ and F is the complementary cumulative value of the normal distribution with mean equal to zero and standard deviation, σ. T_t is calculated by Eq. (2), since M_{min}, M_p and Q are known.

In the following paragraphs of this section, instrumental ($M\geq5.2$, 1911-2009) and historical

(M≥6.0, 464BC-1910) earthquake data are used (Papazachos *et al*., 2010a) to define parameters of time-independent and time-dependent seismicity (intermediate term prediction of strong earthquakes) in the Aegean area (34^0N-43^0N, 19^0E-30^0E). Thus, 127 circular (C, r≤67 km) seismic zones (non overlapping circular regions) have been defined, for which parameters of time-independent seismicity have been calculated and are presented. Also, 120 circular (C, R≤100 km) regions of interacting faults (partly overlapping regions where the TIMAP model is applicable) have been defined, for which parameters of time-dependent seismicity are calculated and applied for a backward test by retrospective prediction of strong (M≥6.0) mainshocks in the Aegean area.

2.1. Definition of circular seismic zones in the Aegean area

Seismic zonation of a broad area is usually based on several geophysical and geological pieces of information, but information concerning the size and the space distribution of earthquakes is essential for such zonation. In high seismicity regions, for which large samples of reliable instrumental and historical seismological data are available, as in the case of the Aegean area, such data can be used to objectively define seismic zones on which studies of time-independent and time-dependent seismicity can be based. In the present work, circular seismic zones have been defined in the Aegean area by the following procedure.

Initially, the circular seismic zone centered at the epicenter, E_1, of the largest known earthquake in the whole Aegean area (34^0N-43^0N, 19^0E-30^0E), with radius, r_1, equal to the half of its expected fault length, $r_1=L_1/2$, was defined. This length is defined by a proper relation between the fault length, L (in km), and the moment magnitude, M, proposed by Papazachos and Papazachou (2003), which holds for the Aegean area:

$$\log L = 0.51 \cdot M - 1.85. \quad (4)$$

All earthquakes of the original catalogue, with epicenters in the circle (E_1, r_1), form the available sample of earthquakes for this first circular seismic zone. This sample of earthquakes is excluded from the original catalogue and the remaining part forms a second "residual" catalogue. The largest earthquake of the new catalogue, as well as its circular focal region (E_2, $r_1=L_2/2$) were then defined. If $(E_1E_2)\geq(r_1+r_2-d)$, where d is a predefined small distance (e.g., d=10 km), the circular focal region (E_2, r_2) is the second circular zone of the Aegean area and the earthquakes of this zone are excluded from the second catalogue to form a third catalogue which is used to define the third seismic zone (E_3, r_3) in the same way. If, however, $(E_1E_2)<(r_1+r_2-d)$, which means that the two regions significantly overlap, the focal region (E_2, r_2) is not considered as a seismic zone, its earthquakes are not excluded from the second catalogue and the next (in size) earthquake of this new catalogue is used as a candidate for a circular zone center. This procedure is continued till the epicenter of each strong (M≥6.0) earthquake of the original catalogue is located in either one of the defined circular seismic zones or is located outside of these zones but has been already tried as a candidate for a zone center.

It must be pointed out that, using the previous procedure, the position of each possible focal region (E_i, r_i) has been examined (by corresponding relations) with respect to the position of each one of the already defined ones. Thus, none of the 127 circular seismic zones finally defined in

this way in the Aegean area has significant overlap with its adjoining seismic zones (see Fig. 1). It must be also taken into account that the fault lengths, calculated on the basis of Eq. (4), for earthquakes with magnitudes 6.0-6.5 range between 16 km and 30 km. Taking into account that the average error for the epicenter determination is of the order of 20 km, we have set the minimum radius of the seismic zones for earthquakes of this magnitude range equal to 25 km. The data used in this study come from the catalogue of Papazachos *et al*. (2010a) and fulfill the following completeness criteria (Papazachos and Papazachou, 2003):

$M \geq 4.0$, 1981-2009 (5)

$M \geq 4.5$, 1964-1980 (6)

$M \geq 5.2$, 1911-1963 (7)

$M \geq 6.5$, 1850-1910 (8)

$M \geq 7.0$, 1700-1849 (9)

where the first three of these relations concern instrumental and the rest concern historical data periods.

The parameters usually needed for estimating time-independent seismicity of a seismic zone are: the magnitude, M_{max}, of the largest known earthquake of the zone and the parameters, a (annual) and b of the Gutenberg-Richter cumulative recurrence relation. The M_{max} is the calculated magnitude of the largest earthquake ever observed in each zone (located at the center of the circular seismic zone). It should be noted that two historical earthquakes have occurred in the Aegean area for which very large magnitudes have been estimated (365 A.D. M=8.3, 1303 M=8.0) These earthquakes have very large repeat times (~1000 years), that are much larger than the repeat times of practical interest and are also much larger than the repeat times of the largest earthquakes (M=7.6) which occurred during the instrumental period in the Aegean area. For this reason, M_{max} was considered equal to 7.8 for the 365 A.D. event and to 7.7 for the 1303 event for the calculation [using Eq. (4)] of the seismic zone radius for these two big earthquakes (r_1=67 km and r_2=60 km, respectively).

For the calculation of the b and a values for each circular seismic zone, the data defined by the completeness Eqs. (5), (6) and (7) have been used. To determine the b value for a certain seismic zone centered at E, all earthquakes that have occurred within R=100 km from E and that fulfill the completeness criteria mentioned previously, were considered. In almost all zones examined, the difference between the minimum and maximum earthquake magnitude used in the calculations was equal to or larger than 1.8 while the number of log$N$-M pairs was larger than four, thus ensuring a fairly reliable b-value estimation. In rare cases, where the latter requirements were not met, R was increased in steps of 5 km. Then, by using this value of b and information for the earthquakes that are defined by Eqs. (5), (6), (7) and are located in the circular seismic zone (E, r), the parameter a (annual) is calculated. The first five columns of Table 1 give the code number n_o, the geographic coordinates of the center $E(\varphi, \lambda)$, the radius r (in km) and the focal

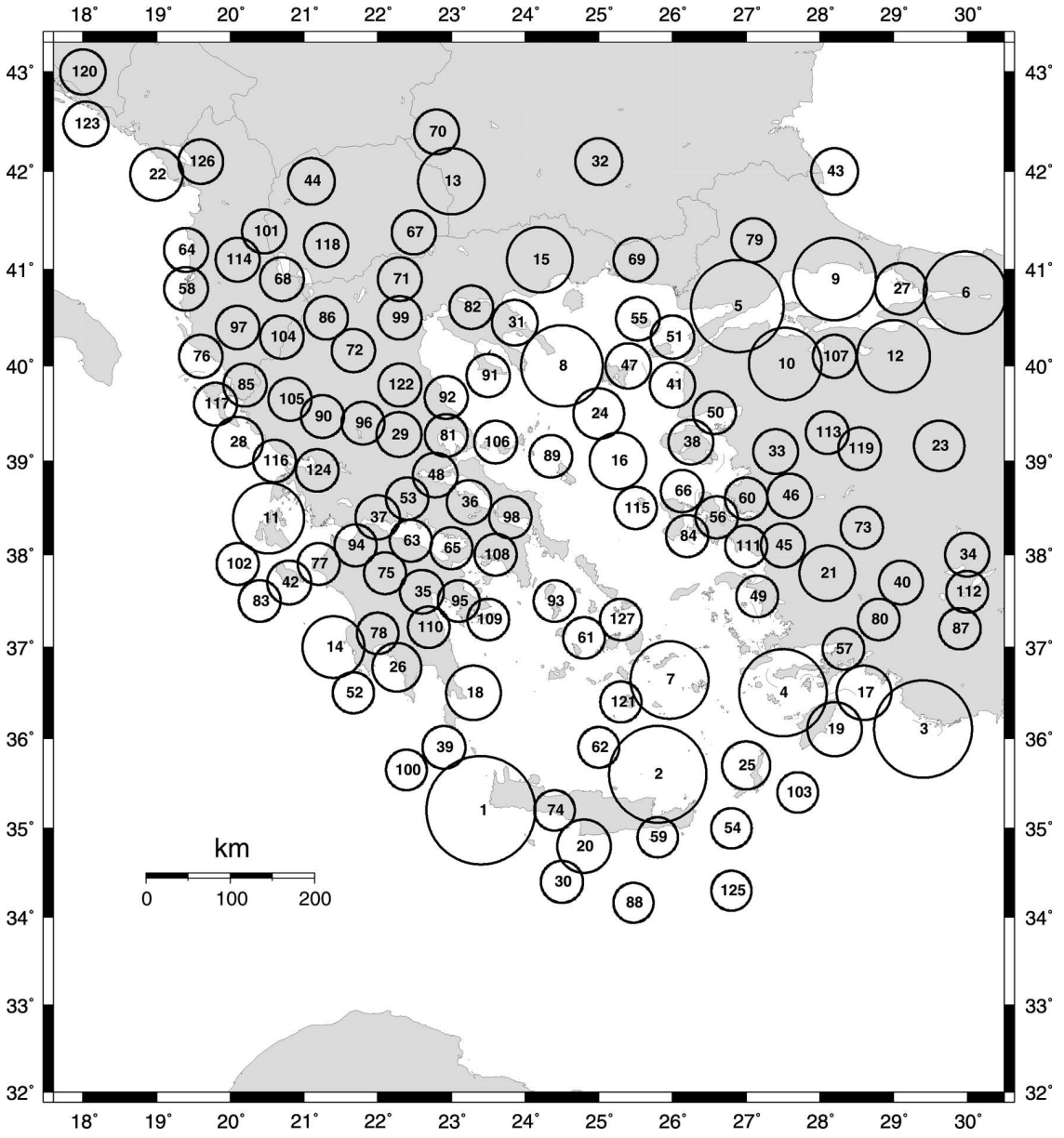

Fig. 1 - The 127 circular seismic zones with focal depths h≤100 km in the Aegean area. Numbers correspond to the code numbers of Table 1 where the seismicity parameters (M_{max}, *a, b*) are given.

depth *h* (in km, *h*=n for *h* 40 km) of the zone. The next four columns give the year of occurrence, *Yr*, and the magnitude, M_{max}, of the largest earthquake of the zone as well as the values of the parameters *a* (for one year) and *b.*

2.2. Declustering of the original data

Earthquakes located in each of the 127 seismic zones are clustered also in time, since several

Table 1 - Circular seismic zones and regions of interacting faults in the Aegean area. In the first five columns the code number n_o, the geographic coordinates of the center $E(\varphi, \lambda)$, the radius r (in km) and the maximum focal depth h (in km, n for shallow depths) are given. In the next four columns the year, Yr, of occurrence and the magnitude, M_{max}, of the largest observed earthquake in the zone are given along with the parameters a (annual) and b. The next six columns list parameters for the regions of interacting faults, namely, the radius R_q (in km) of each region, the number N_q of the interevent times, the Q value of Eq. (2) and the corresponding standard deviation σ_q, the W value of Eq. (3) and its standard deviation σ_w.

n_o	$\varphi°_n$	$\lambda°_E$	r (km)	h (km)	Yr	M_{max}	a	b	R_q (km)	N_q	Q	σ_q	W	σ_w
1	35.2 0	23.4 0	67	n	365	7.8	6.38	1.28	95	21	-2.12	0.19	3.79	0.49
2	35.60	25.80	60	61	1856	7.7	5.88	1.25	100	49	-2.19	0.26	4.06	0.48
3	36.10	29.40	60	n	1303	7.7	4.41	0.98	75	23	-1.81	0.22	3.80	0.35
4	36.50	27.50	53	100	1926	7.6	5.47	1.09	95	42	-2.08	0.25	3.90	0.45
5	40.62	26.88	53	n	1912	7.6	3.25	0.81	100	65	-2.14	0.31	4.17	0.41
6	40.76	29.97	47	n	1999	7.5	3.78	0.88	30	6	-1.48	0.09	4.39	0.52
7	36.64	25.96	47	n	1956	7.5	4.68	1.04	-	-	-	-	-	-
8	40.00	24.50	47	n	1905	7.5	4.47	0.98	100	53	-2.25	0.19	4.24	0.40
9	40.90	28.20	47	n	740	7.5	3.88	0.99	100	29	-1.82	0.15	3.48	0.44
10	40.02	27.53	42	n	1953	7.4	3.50	0.83	100	52	-2.14	0.29	4.29	0.65
11	38.39	20.52	42	n	1867	7.4	6.00	1.15	100	59	-2.18	0.23	4.07	0.28
12	40.10	29.00	42	n	1855	7.4	4.99	1.20	95	27	-1.96	0.20	3.75	0.35
13	41.90	23.00	37	n	1904	7.3	4.15	1.07	100	9	-1.50	0.23	3.58	0.51
14	37.00	21.40	37	n	1886	7.3	5.53	1.19	95	60	-2.11	0.21	3.94	0.30
15	41.10	24.20	37	n	1829	7.3	3.03	0.93	85	7	-1.69	0.08	3.35	0.40
16	39.00	25.26	33	n	1981	7.2	4.53	1.05	75	22	-2.03	0.28	3.98	0.76
17	36.50	28.60	33	n	1957	7.2	4.63	1.05	95	53	-1.90	0.32	4.01	0.53
18	36.50	23.30	33	100	1926	7.2	3.74	0.91	100	37	-1.93	0.37	4.04	0.30
19	36.10	28.20	33	n	1513	7.2	4.93	1.13	95	50	-2.13	0.28	3.92	0.60
20	34.80	24.80	33	n	448	7.2	5.85	1.26	100	34	-2.05	0.23	3.90	0.35
21	37.80	28.10	33	n	-27	7.2	4.53	1.16	95	41	-2.09	0.16	3.15	0.07
22	41.97	19.00	30	n	1979	7.1	5.21	1.17	90	16	-1.75	0.18	4.04	0.47
23	39.16	29.62	30	n	1970	7.1	5.40	1.16	100	15	-1.82	0.14	4.05	0.58
24	39.50	25.00	30	n	1968	7.1	4.13	1.00	90	68	-2.13	0.31	4.19	0.65
25	35.70	27.00	30	n	1948	7.1	5.47	1.20	95	29	-2.09	0.20	3.87	0.31
26	36.78	22.26	30	n	1927	7.1	4.16	1.04	85	52	-2.10	0.26	3.98	0.31
27	40.80	29.10	30	n	1766	7.1	3.86	0.94	95	49	-1.75	0.33	3.94	0.28
28	39.20	20.10	30	n	1743	7.1	5.22	1.23	85	31	-2.00	0.14	3.25	0.16
29	39.28	22.29	26	n	1954	7.0	3.91	0.97	85	21	-2.25	0.20	3.97	0.50
30	34.40	24.50	26	n	1952	7.0	5.19	1.22	90	34	-2.05	0.16	3.90	0.46
31	40.45	23.86	26	n	1932	7.0	4.12	0.98	100	53	-2.08	0.23	3.60	0.32
32	42.10	25.00	26	n	1928	7.0	2.92	0.80	-	-	-	-	-	-
33	39.10	27.40	26	n	1919	7.0	4.45	1.14	95	23	-2.03	0.15	3.77	0.57

Table 1 - continued.

n_o	$\varphi°_n$	$\lambda°_E$	r (km)	h (km)	Yr	M_{max}	a	b	R_q (km)	N_q	Q	σ_q	W	σ_w
34	38.00	30.00	26	n	1914	7.0	4.63	1.09	100	19	-1.77	0.40	3.78	0.43
35	37.60	22.60	26	90	1898	7.0	4.07	1.05	100	41	-2.20	0.12	3.94	0.26
36	38.56	23.24	26	n	1894	7.0	4.29	1.07	100	41	-2.15	0.14	3.43	0.53
37	38.40	22.00	26	80	1889	7.0	5.22	1.14	100	36	-2.26	0.15	3.54	0.40
38	39.20	26.25	26	n	1867	7.0	4.40	1.08	100	59	-1.99	0.23	3.51	0.47
39	35.90	22.90	26	n	1717	7.0	4.43	1.13	85	35	-1.98	0.28	3.88	0.32
40	37.70	29.10	26	n	1702	7.0	4.95	1.18	35	10	-1.56	0.09	3.29	0.34
41	39.80	26.00	26	n	1672	7.0	3.57	1.03	100	68	-2.08	0.22	3.39	0.31
42	37.70	20.80	26	n	1633	7.0	5.61	1.18	50	48	-2.07	0.12	3.57	0.34
43	42.00	28.20	26	n	544	7.0	1.27	0.80	-	-	-	-	-	-
44	41.90	21.10	26	n	518	7.0	4.20	1.13	85	21	-1.80	0.12	3.59	0.26
45	38.10	27.50	26	n	47	7.0	5.10	1.20	100	53	-2.12	0.20	3.44	0.17
46	38.63	27.59	26	n	17	7.0	4.66	1.16	100	43	-2.10	0.16	3.42	0.37
47	40.00	25.40	26	n	-197	7.0	3.76	1.00	95	67	-2.04	0.34	4.18	0.32
48	38.85	22.78	26	n	-426	7.0	4.05	1.06	100	42	-2.25	0.22	3.79	0.52
49	37.55	27.15	25	n	1955	6.9	5.34	1.27	100	24	-2.02	0.19	4.07	0.31
50	39.51	26.57	25	n	1944	6.9	3.41	0.91	100	65	-2.02	0.17	3.70	0.24
51	40.30	26.00	25	n	1859	6.9	4.11	0.95	100	72	-2.08	0.27	3.71	0.24
52	36.50	21.67	25	n	2008	6.8	5.01	1.14	100	42	-2.09	0.19	3.89	0.61
53	38.60	22.40	25	78	1965	6.8	4.29	1.04	75	34	-2.00	0.15	3.73	0.50
54	35.00	26.80	25	n	1922	6.8	6.24	1.37	80	26	-2.11	0.11	3.48	0.37
55	40.49	25.53	25	n	1893	6.8	4.27	1.10	95	44	-1.94	0.32	3.78	0.37
56	38.40	26.60	25	n	1883	6.8	5.35	1.28	95	42	-2.23	0.17	3.66	0.25
57	36.98	28.32	25	n	1869	6.8	4.35	1.03	85	27	-1.99	0.16	3.63	0.41
58	40.80	19.40	25	n	1851	6.8	5.23	1.26	45	14	-1.71	0.10	3.38	0.18
59	34.90	25.80	25	n	1780	6.8	6.10	1.38	95	39	-2.13	0.19	3.43	0.14
60	38.60	27.00	25	n	1739	6.8	4.66	1.16	85	51	-2.12	0.18	3.73	0.24
61	37.10	24.80	25	n	1733	6.8	2.87	1.04	-	-	-	-	-	-
62	35.90	25.00	25	61	1665	6.8	3.86	1.00	100	31	-2.23	0.26	4.29	0.34
63	38.15	22.45	25	n	1402	6.8	4.78	1.09	50	35	-2.03	0.18	3.73	0.28
64	41.20	19.40	25	n	1273	6.8	4.92	1.16	90	33	-2.02	0.17	3.29	0.19
65	38.07	23.00	25	n	1981	6.7	4.82	1.06	65	38	-2.12	0.11	3.80	0.49
66	38.68	26.13	25	n	1949	6.7	4.71	1.12	85	37	-1.99	0.30	4.01	0.33
67	41.38	22.49	25	n	1931	6.7	4.23	1.07	60	8	-1.56	0.11	3.60	0.43
68	40.90	20.70	25	n	1911	6.7	4.89	1.13	100	32	-2.10	0.26	3.68	0.37
69	41.10	25.50	25	n	1784	6.7	3.87	1.23	100	17	-1.99	0.28	3.31	0.35
70	42.40	22.80	25	n	1641	6.7	4.73	1.42	-	-	-	-	-	-

Table 1 - continued.

n_o	$\varphi°_n$	$\lambda°_E$	r (km)	h (km)	Y_r	M_{max}	a	b	R_q (km)	N_q	Q	σ_q	W	σ_w
71	40.90	22.30	25	n	1395	6.7	3.84	1.01	100	17	-1.84	0.17	3.30	0.31
72	40.16	21.67	25	n	1995	6.6	5.37	1.23	100	21	-1.94	0.10	3.68	0.42
73	38.29	28.57	25	n	1969	6.6	4.83	1.22	100	33	-1.91	0.19	3.58	0.34
74	35.20	24.40	25	80	1948	6.6	5.11	1.18	100	44	-2.03	0.22	3.72	0.35
75	37.80	22.10	25	80	1925	6.6	4.51	1.11	70	42	-2.01	0.14	3.62	0.44
76	40.10	19.60	25	n	1893	6.6	5.73	1.29	95	27	-2.05	0.25	3.45	0.48
77	37.90	21.20	25	n	1873	6.6	5.42	1.17	90	63	-2.19	0.19	4.08	0.29
78	37.15	22.00	25	n	1846	6.6	4.56	1.09	100	46	-2.16	0.24	3.96	0.34
79	41.30	27.10	25	n	1689	6.6	1.47	0.80	100	34	-1.87	0.46	4.26	0.31
80	37.30	28.80	25	n	241	6.6	4.89	1.21	65	15	-1.94	0.07	3.23	0.24
81	39.27	22.93	25	n	1980	6.5	4.44	1.00	85	31	-2.05	0.19	3.93	0.40
82	40.61	23.27	25	n	1978	6.5	4.33	1.02	100	23	-1.95	0.22	4.00	0.35
83	37.50	20.40	25	n	1976	6.5	5.34	1.19	100	61	-2.17	0.22	3.88	0.18
84	38.20	26.20	25	n	1881	6.5	5.45	1.40	90	33	-1.93	0.18	3.52	0.15
85	39.80	20.20	25	n	1854	6.5	5.61	1.30	100	38	-2.00	0.22	3.41	0.24
86	40.50	21.30	25	n	1812	6.5	4.20	1.12	65	28	-1.86	0.20	3.75	0.26
87	37.20	29.90	25	n	417	6.5	4.76	1.18	100	16	-1.90	0.36	3.69	0.33
88	34.16	25.47	25	n	2009	6.4	6.25	1.39	70	26	-1.85	0.15	3.46	0.24
89	39.05	24.35	25	n	2001	6.4	4.42	1.02	100	32	-2.13	0.29	3.77	0.38
90	39.47	21.25	25	n	1967	6.4	4.89	1.20	90	28	-1.97	0.18	3.58	0.31
91	39.90	23.50	25	n	1923	6.4	3.56	0.97	100	41	-2.19	0.17	3.72	0.27
92	39.67	22.93	25	n	1905	6.4	3.51	0.98	70	15	-2.05	0.07	3.64	0.26
93	37.50	24.40	25	n	1891	6.4	4.93	1.41	-	-	-	-	-	-
94	38.10	21.70	25	n	1804	6.4	4.88	1.15	80	42	-2.14	0.14	3.58	0.40
95	37.50	23.10	25	n	1769	6.4	3.99	1.06	100	30	-2.11	0.15	3.93	0.18
96	39.40	21.80	25	n	1735	6.4	3.91	1.05	100	18	-2.22	0.16	4.17	0.60
97	40.40	20.10	25	n	1701	6.4	4.95	1.21	80	41	-2.09	0.28	3.82	0.29
98	38.40	23.80	25	n	1417	6.4	5.05	1.24	85	21	-1.89	0.14	3.49	0.30
99	40.50	22.30	25	n	1211	6.4	3.99	1.07	100	22	-1.93	0.20	3.53	0.58
100	35.65	22.39	25	65	1992	6.3	5.80	1.36	80	31	-1.92	0.18	3.51	0.50
101	41.39	20.46	25	n	1967	6.3	5.00	1.14	80	38	-1.93	0.18	3.57	0.30
102	37.90	20.10	25	n	1962	6.3	5.52	1.15	80	66	-2.11	0.22	3.95	0.42
103	35.40	27.70	25	n	1922	6.3	6.13	1.32	50	28	-1.82	0.19	3.46	0.26
104	40.30	20.70	25	n	1919	6.3	5.00	1.21	100	36	-2.11	0.26	3.31	0.20
105	39.65	20.81	25	n	1898	6.3	5.62	1.32	100	32	-1.97	0.17	3.22	0.13
106	39.20	23.60	25	n	1868	6.3	4.98	1.13	85	37	-1.99	0.16	3.48	0.27
107	40.10	28.20	25	n	1850	6.3	3.55	0.97	50	10	-1.84	0.11	3.38	0.39

Table 1 - continued.

n_o	$\varphi°_n$	$\lambda°_E$	r (km)	h (km)	Yr	M_{max}	a	b	R_q (km)	N_q	Q	σ_q	W	σ_w
108	38.00	23.60	25	n	1705	6.3	4.40	1.14	100	35	-2.07	0.12	3.60	0.19
109	37.30	23.50	25	n	1457	6.3	2.88	0.91	100	35	-2.02	0.16	3.83	0.28
110	37.22	22.69	25	75	2008	6.2	2.94	0.86	100	38	-2.30	0.13	3.48	0.24
111	38.09	27.00	25	n	1992	6.2	5.54	1.28	100	48	-2.07	0.19	3.63	0.21
112	37.60	30.00	25	n	1971	6.2	4.82	1.14	100	11	-1.95	0.40	3.79	0.43
113	39.30	28.10	25	n	1942	6.2	4.37	1.03	90	23	-1.96	0.18	3.66	0.30
114	41.10	20.10	25	n	1907	6.2	4.99	1.16	85	51	-2.08	0.23	3.76	0.33
115	38.50	25.50	25	n	1890	6.2	4.64	1.14	95	21	-1.90	0.22	4.26	0.66
116	39.00	20.60	25	n	1826	6.2	5.33	1.15	100	46	-2.14	0.24	4.08	0.30
117	39.60	19.80	25	n	1666	6.2	5.66	1.39	85	27	-1.86	0.20	3.19	0.17
118	41.25	21.30	25	n	1994	6.1	3.86	1.07	85	25	-1.91	0.19	3.50	0.18
119	39.13	28.54	25	n	1969	6.1	4.68	1.09	100	19	-1.98	0.24	3.69	0.32
120	43.00	18.00	25	n	1927	6.1	3.76	1.06	100	6	-1.47	0.31	3.30	0.29
121	36.40	25.30	25	n	1919	6.1	3.29	0.87	90	19	-2.08	0.14	4.06	0.25
122	39.80	22.30	25	n	1766	6.1	3.00	0.96	75	21	-1.94	0.10	3.72	0.83
123	42.48	18.04	25	n	1996	6.0	3.13	0.93	60	10	-1.54	0.17	3.34	0.22
124	38.90	21.18	25	n	1921	6.0	5.00	1.15	55	28	-1.98	0.10	3.55	0.25
125	34.30	26.80	25	n	1910	6.0	6.14	1.42	65	19	-1.73	0.08	3.14	0.05
126	42.10	19.60	25	n	1905	6.0	4.78	1.18	100	34	-1.84	0.17	3.84	0.59
127	37.30	25.30	25	n	-50	6.0	1.71	0.81	-	-	-	-	-	-

seismic sequences that include mainshocks and their associated shocks (preshocks, postshocks) can be found in all zones. Declustering of the earthquakes corresponds to the definition of the mainshocks of each region by excluding the shocks associated with each mainshock. By definition associated shocks occur within a certain space and time window from the mainshock. Karakaisis *et al*. (2010) used data for the Aegean area to show that, by excluding associated shocks which occur within a distance $\delta x \leq 50$ km from the epicenter and within a time interval $\delta t = \pm 8.5$ years from the origin time of a mainshock, a ratio $\sigma/T=0.5$ is obtained for the mean repeat time, T, and its standard deviation, σ. That is, when declustering is performed by using these space and time windows, the remaining mainshocks exhibit quasi-periodic behavior (Kagan and Jackson, 1991). On the basis of the previous results, the following procedure was applied to decluster the original catalogue (defined by Eqs. (5) to (9) and obtain a mainshock catalogue. Declustering starts from the first seismic zone, centered at the epicenter of the largest known earthquake for the whole Aegean area. This earthquake is considered as the first mainshock and its associated shocks that have occurred in the defined space ($\delta x \leq 50$ km) and time ($\delta t \pm 8.5$ years) windows are excluded from the original catalogue. Then, the largest earthquake of the remaining earthquakes in the same seismic zone is considered as the second mainshock and its associated shocks for the same space and time windows ($\delta x \leq 50$ km, $\delta t \pm 8.5$ years) are excluded

from the original catalogue.

This procedure is repeated until all mainshocks with $M \geq 5.2$ of this first seismic zone are selected. The same procedure is applied for the second circular seismic zone by using the remaining part of the original catalogue, after excluding the mainshocks of the first focal region and their associated shocks. Repeating this procedure for all the zones, a new catalogue of mainshocks with $M \geq 5.2$ is compiled for the whole Aegean area.

2.3. Determination of regions of interacting faults

Each region for which the mainshock generation fulfills Eqs. (1) and (3) has been considered as a "region of interacting faults". Centers, E, of seismic zones defined for the Aegean area (section 2.1) are also considered as centers of circular regions of interacting faults (E, R_q) for this area. Each circular region was considered as a region of interacting faults, if it included the epicenters of a complete sample of mainshocks that defines at least $N \geq N_q$ inter-event times (e.g., N_q=4), and the mean value of Q [calculated by Eq. (1)] for this region had a small enough standard deviation, σ_q, or a large enough corresponding number of inter-event times, N_q, so that the ratio N_q/σ_q obtained its maximum value with respect to its values in all other circular regions (E, $R \leq 100$ km). To define such a region, circles centered at E (the center of the corresponding circular seismic zone) and with a radius, R_i, varying between 15 km and 100 km (with a certain step, e.g., δR=5 km) were considered and the mean value of Q and its standard deviation, σ_i, are calculated for each of these circles with $N \geq 4$. The radius, R_q, which corresponded to the highest ratio N_q/σ_q, was taken as the radius of the corresponding circular region, (E, R_q), of interacting seismic faults. In this way, 120 circular regions of interacting seismic faults have been determined for the whole Aegean area. Available information (M_{min}, M_p, M_f) for each of these 120 regions of seismic faults has been used to calculate the mean value of W of Eq. (2) and the corresponding standard deviation, σ_w. In Table 1, the values of R_q(in km), N_q, Q, σ_q, W, σ_w, are listed.

2.4. A backward test of the model

The TIMAP model was applied to calculate the probabilities [by Eqs. (1) and (3)] and the magnitude [by Eq. (2)] for the strong ($M \geq 6.0$) mainshocks expected in each one of the 120 circular fault regions during each of the following decades 1970-1979, 1980-1989, 1990-1999, 2000-2009. These decades were selected because a dense network of seismic stations was in operation in the Aegean area and for this reason the available relative data are of the same (high) quality as the data of the next decade (2010-2019) for which predictions of ensuing mainshocks are attempted in section 4. In this backward test the M_{min} value and the magnitude, M_p, of the previous mainshock with origin time t_p are needed to calculate the probability, P_t, and the M_f for each faults' region and for each of the four decades. M_{min} is predefined (e.g., M_{min}=6.0), hence M_p and t_p are the magnitude and the occurrence time of the last strong ($M \geq 6.0$) mainshock that occurred before the examined decade in each region.

The main goal of this backward test of the TIMAP model was to define the percentage of false alarms and the percentage of unpredictable mainshocks. In order to perform this test, the center, K_1, of the first group is the geographical point, C_1, with the highest probability in the whole Aegean area and the first group is formed by all points, C, with $P_t > 0.50$, which are in the circle (K_1, R_1) with radius R_1 equal to R_q corresponding to the circle with center C_1. As first predicted

epicenter, E_1, we take the center K_1 but as first predicted probability, P_1, the average of the three highest probabilities (>0.50) of the first group is taken. As second predicted epicenter, E_2, is considered the center, C_2, outside the circle (K_1, R_1) with the largest probability in respect of the probabilities of all other C points outside this circle. The second group is formed by the C points with P_t>0.50 which are in the circle (K_2, R_2) with radius R_2 equal to R_q corresponding to C_2. As second probability, P_2, the average of the three highest corresponding values of the group was also used. This procedure is continued till all points, C, with P_t>0.50 are considered. It is understood that in this procedure the position of every new defined center, K, must be located outside of all previously defined circular regions (K_i, R_i). These regions, however, can overlap, that is, some points C with P_t >0.50 may belong to more than one group.

The location of the epicenters, E, of each of the occurred strong (M≥6.0) mainshocks of the decade was examined with respect to all the defined circular regions (K_i, R_i) and if the mainshock was located in more than one such region it was considered as belonging to the region with the highest probability. In this way, a mainshock located in at least one of these regions (for which P_t >0.50) is considered as predictable by the model and a mainshock which is not located in any of these regions is considered as unpredictable. The ratio of the number of unpredictable strong (M≥6.0) mainshocks to the number of all mainshocks that occurred during a decade in an area (e.g., Aegean) is the failure ratio. This ratio decreases with increasing radius. For R_i =130 km this ratio becomes very small. For this reason in the present study (which concerns the Aegean area), we selected R_i=130 km for which the failure ratio is very small (~0.02).

The false alarm ratio is also of interest, as it too decreases with increasing R_i but its rate of decrease is low and for R_i=130 km this ratio is relatively high (~0.40) for the Aegean area. This is the main handicap of the TIMAP model. For this reason, this model is applied here in combination with the D-AS model for which a small (~0.10) false alarm ratio has been estimated (Papazachos *et al*., 2006). It must be, however, mentioned that several cases of false alarms for each of the decades considered in the present backward test concern mainshocks that occurred during the following decade. On the other hand, the model has the important advantage that the failure ratio is very small.

3. The Decelerating-Accelerating Seismic Strain (D-AS) Model

Papazachos *et al*. (2006) developed the D-AS model for intermediate-term prediction of strong mainshocks by taking into consideration the relevant published information on the observed decelerating and accelerating precursory seismicity, which is based on seismicity patterns that preceded globally occurring strong (M>6.3) mainshocks. This is based upon recent global (since 1980) data. A very distinct pattern of seismicity is the one which is formed by precursory seismic excitation in a broad region and reduced seismicity in a narrower focal region of an ensuing mainshock, which has been described as “doughnut pattern” by Mogi (1969). An additional relative research (Tocher, 1959; Knopoff *et al*., 1996; Brehm and Braile, 1999; Robinson, 2000; Tzanis *et al*., 2000; Ben-Zion and Lyakhovsky, 2002; Papazachos *et al*., 2005a, among others) has shown that precursory seismic excitation in the broad (critical) region is characterized by accelerating generation of intermediate magnitude preshocks. This is expressed by power-law relations of the form:

$$S(t) = A + B(t_c - t)^m \tag{10}$$

where $S(t)$ is the time variation of the cumulative Benioff strain (sum of the square root of seismic energy), t_c is the origin time of the ensuing mainshock and A, B, m are parameters calculated by the available data with $m<1$ and B negative (Bufe and Varnes, 1993). Papazachos *et al*. (2005b) used global data to show that intermediate magnitude preshocks in the narrow (seismogenic) region form a decelerating pattern and the time variation of the precursory cumulative Benioff strain also obeys a power-law [Eq. (10)] but with a power value larger than a unit ($m>1$).

Forward tests of the D-AS model have been also performed by attempting predictions of future mainshocks. Predictions of two ensuing mainshocks in the Aegean area were made successfully. The first such prediction concerns the strong (M=6.9) mainshock that occurred on January 8, 2006 near Cythera Island in the southwestern part of the Hellenic Arc (Papazachos *et al*., 2002, 2007). The second prediction concerns the strong (M=6.4) mainshock that occurred on July 15, 2008 near Rhodes Island in the eastern part of the Hellenic Arc (Papazachos and Karakaisis, 2008; Papazachos *et al*., 2009). Very recently, all this information and the results of the D-AS model for already occurring recent (1980-2008) strong ($M\geq6.0$) mainshocks in seven global seismotectonic regimes led to some improvements in the relations that are used to predict the time of origin, t_c, of the moment magnitude, M, and of the epicenter coordinates, $E(\varphi, \lambda)$, of strong ($M\geq6.0$) mainshocks. These refined relations are as follows.

The estimation (prediction) of the origin time, t_c (in years), is based on the relations:

$$\log\left(t_c - t_{sd}\right) = 2.95 - 0.31\log s_d, \quad \sigma = 0.12 \tag{11}$$

$$\log\left(t_c - t_{sa}\right) = 4.60 - 0.57\log s_a, \quad \sigma = 0.10 \tag{12}$$

where t_{sd} and t_{sa} are the start times of the decelerating and accelerating seismic sequence, respectively, s_d and s_a are the rates of decelerating and accelerating seismic strain release (Papazachos *et al*., 2006) and σ are the corresponding standard deviations. As origin time of an ensuing mainshock is considered the average of the two values calculated by Eqs. (11) and (12).

The calculation (prediction) of the moment magnitude, M, of an ensuing mainshock is made by the relations:

$$\log a = 0.23M - 0.14\log s_d + 1.40, \quad \sigma = 0.10 \tag{13}$$

$$\log R = 0.42M - 0.30\log s_a + 1.25, \quad \sigma = 0.15 \tag{14}$$

where a (in km) is the radius of the circular region where the epicenters of the decelerating preshocks are located (seismogenic region) and R (in km) is the radius of the circular region where the epicenters of the accelerating preshocks are located (critical region). The average

magnitude value calculated by these two relations is considered as the predicted magnitude of the ensuing mainshock.

The location of the epicenter, $E(\varphi, \lambda)$, of an ensuing mainshock is based on properties of decelerating and accelerating preshocks and on the location of previously occurring mainshocks. In particular, the geographic coordinates of the epicenter of an ensuing mainshock are the geographic mean (mean latitude, mean longitude) of four points (*D*, *L*, *K* and *G*).

D is a distinct point in the region of decelerating preshocks and to locate it, several properties of the geographic distribution of these preshocks are taken into consideration (Papazachos *et al*., 2006). A corresponding distinct point, *A*, based on properties of accelerating preshocks has been also defined.

L is defined by properties of both decelerating and accelerating preshocks which precede a mainshock. In particular, two quality indices q_d and q_a, which are measures of the degree of deceleration and acceleration, respectively, of the Benioff strain, have been defined (Papazachos *et al*., 2006). These indices take their largest values (q_{df}, q_{aq}) at the geometrical centers (*F, Q*) of the region of decelerating preshocks (seismogenic region) and of the region of accelerating preshocks (critical region), respectively. Global data show that these indices take smaller values (q_{de}, q_{ae}) at the mainshock epicenter and that:

$$\frac{q_{de}+q_{ae}}{q_{df}+q_{aq}} = 0.45 \pm 0.13. \qquad (15)$$

The geographical mean of the three geographic points that better fulfill Eq. (15) define *L*.

K is the geographical mean of the epicenters of the three largest known mainshocks that occurred in the past within the circle with center *D* and radius 130 km, which is the mean radius of the seismogenic region. Finally, *G* is that of the two points where the line *DA* intersects the circle (*D*, *R*=130 km) which is closer to the geographical mean, V_f, of the epicenter of decelerating preshocks. The uncertainties in the estimated parameters by the D-AS model are: ±2.5years for the origin time, ±0.3 for the magnitude and ≤150 km for the epicenter, with an about 80% probability (Papazachos *et al*., 2006, 2010b).

3.1. Probabilities for random occurrence of the predicted mainshocks

Calculation of the probability for random occurrence of each one of the six mainshocks (see next section) within the predicted space, time and magnitude windows is necessary because if this probability is high, compared to the D-AS model probability (80%), the corresponding prediction is practically meaningless. Calculation of probability for random occurrence is usually based on the assumption that the magnitudes of the earthquakes of the sample used are distributed according to the Gutenberg-Richter (G-R) recurrence law and their times follow a simple Poisson distribution.

To obtain reliable estimations of random probabilities, complete samples of earthquakes with $M \geq 5.2$ are considered. These earthquakes occurred during the instrumental period (January 1, 1911- October 1, 2009) in each one of the six circles (*E*, R*=120 km). Using these data sets all shallow shocks (h≤100 km) in each predicted circular region were considered and the well known

G-R relation was fitted to the data in the least-squares' sense:

$$\log N_t = a_t - bM \tag{16}$$

where N_t is the number of shocks with magnitude M or larger which correspond to 99 years duration (1911-2009). Reduction of the constant of Eq. (16) to its annual value, a, is obtained by $a=a_t$ - log99. The probability, $P_r(M)$, for random occurrence of an earthquake with magnitude M or larger during the prediction time window t (=5 years) is given by the relation:

$$\mathrm{P_r} = 1 - \exp\left(-\frac{t}{T}\right) \tag{17}$$

where $T=10^{bM-a}$. Since the predicted magnitude window by the D-AS model in the Aegean is $M\pm0.3$, the difference in the probabilities obtained by Eq. (17) for the two magnitude limits, allows us to assess the probability for random occurrence of the earthquake in the predicted magnitude window.

The calculated probabilities for random occurrence are listed, for each prediction area, in the last column of Table 2. These results show a relatively low ratio (~0.19) of random/D-AS model probabilities, verifying the significance of the corresponding predictions.

For cases with relatively high random probabilities, a more elaborate evaluation of the model performance is needed by applying more sophisticated techniques. We have, already, developed an algorithm based on such techniques (Papazachos *et al*., 2009). This algorithm can be applied for the finally observed distribution of the strong ($M\geq6.3$) mainshocks in the Aegean area during the period 2010-2017.

4. A forward test of both models

Obviously, forward tests give much more reliable results than backward tests. This is the basic reason why forward tests of the D-AS and TIMAP models are performed in the present section. A serious shortcoming of these forward tests is that it is necessary for the prediction period to elapse in order to evaluate their performance. However, due to the fact that the two models are based on different principles and data (interevent times of mainshocks, behavior of preshocks), comparison of their results concerning estimation (prediction) of future strong mainshocks can give evidence on their reliability.

By applying the D-AS model in the Aegean area, six regions of decelerating and six corresponding regions of accelerating seismic strain have been identified. Three of these regions were previously identified by using data up to October 2007 and their circular seismogenic and critical regions, as well as the corresponding time variation of the decelerating and accelerating seismic strain, $S(t)$, (Benioff graphs) have been already published [Fig. 3 in Papazachos *et al*. (2009)]. Information for the additional three cases is given in Fig. 2. By using data up to September 30, 2009 the origin time, magnitude and epicenter coordinates of all these six probably

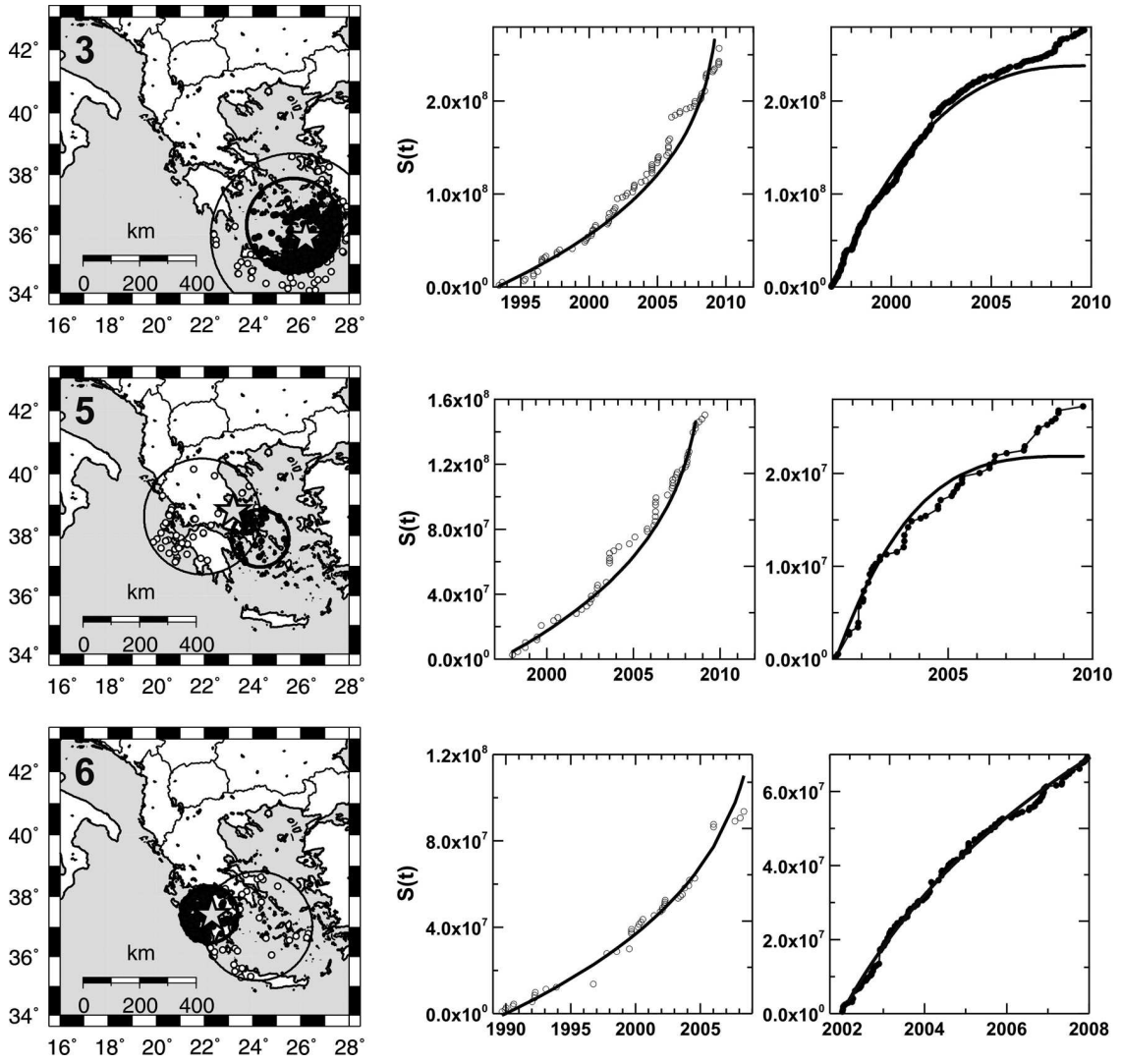

Fig. 2 - Information on the decelerating-accelerating seismicity in three regions of the Aegean area. Dots are epicenters of decelerating shocks which are included in the circular seismogenic region and small open circles are epicenters of accelerating shocks which are included in the circular critical region. The time variations of the accelerating and decelerating Benioff strain, $S(t)$, are shown on the right of each of the three cases. The best-fit lines of the time variation of the Benioff strain which follow a power-law [Eq. (1)] are also shown. Numbers (3, 5, 6) correspond to the code numbers of Table 2.

ensuing mainshocks have been estimated (predicted) by the D-AS model. The six epicenters, E_d, the corresponding origin times, t_d, and magnitudes, M_d, are listed in Table 2.

The procedure described in section 2.4 to retrospectively predict epicenters and probabilities for strong ($M \geq 6.0$) mainshocks occurred in the previous four decades by the TIMAP model, is also applied in the present section, to estimate (predict) these parameters (E_t, P_t) for strong ($M \geq 6.0$) mainshocks probably ensuing in the next decade (1.1.2010-31.12.2019). Nineteen such mainshocks ($M_t \geq 6.0$, $P_t > 0.5$) have been identified. Six of these epicenters, E_t, are near the

Table 2 - Estimated (predicted) origin times, t_d, epicenter coordinates, $E_d(\varphi, \lambda)$ and magnitudes, M_d, by the D-AS model for six regions in the Aegean area. $E_t(\varphi, \lambda)$ and P_t are the epicentres and the probabilities estimated (predicted) by the TIMAP model for the generation of strong mainshocks in these six regions during the decade 2010-2019. t_c*, E*(φ, λ) and M* are the finally adopted parameters for the origin time (with uncertainty ≤2.5 years), the epicenter (with uncertainty ≤120 km) and the magnitude (with uncertainty ≤0.3) of the six probably ensuing mainshocks. The last column lists the probability, P_r, for random occurrence of each mainshock in the corresponding time, space and magnitude windows.

Region	t_d	$E_d(\varphi,\lambda)$	M_d	$E_t(\varphi,\lambda)$	P_t	t_c*	E*(φ,λ)	M*	P_r
1. Albania-Greece border	2012.7	39.8, 20.4	6.7	40.2, 20.9	0.81	2012.7	40.0, 20.7	6.7	0.13
2. N. Aegean	2014.2	39.6, 23.7	7.2	39.8, 23.8	0.74	2014.2	39.7, 23.8	7.2	0.09
3. S. Aegean	2013.5	35.6, 25.5	7.0	35.8, 25.5	0.75	2013.5	35.7, 25.5	7.0	0.11
4. NE borders of Greece	2012.7	39.4, 26.1	6.4	39.6, 26.9	0.84	2012.7	39.5, 26.5	6.4	0.24
5. Central Greece	2014.9	38.8, 23.5	6.5	38.9, 22.8	0.85	2014.9	38.8, 23.1	6.5	0.29
6. SW Greece	2014.7	37.3, 22.2	6.5	37.2, 22.7	0.83	2014.7	37.3, 22.5	6.5	0.36

corresponding epicenters, E_d, determined by the D-AS model (their distances are smaller than 120 km, which is the uncertainty of the location indicated by the D-AS model in the Aegean). The epicenter, E_t (φ, λ), and the probability, P_t, estimated for these six probably ensuing mainshocks are listed in Table 2. In this table, the finally adopted (predicted), t_c*, E*(φ, λ) and M* are also listed on the basis of information given by both models. t_c* is the origin time estimated by the D-AS model, E*(φ, λ) is the geographical mean (mean latitude, mean longitude) of the two epicentres estimated by the two models and M* is equal to the magnitude calculated by the D-AS model. The uncertainties of these finally adopted parameters are ±2.5 years for the origin time, δx≤120 km for the epicenter and ±0.3 for the magnitude, with an about 80% probability.

It should be noted that the additional 13 strong earthquakes defined by the TIMAP model may be mainshocks for which no decelerating-accelerating precursory pattern has yet been identified or they could be false alarms.

5. Discussion and conclusions

The TIMAP regional model employs interevent times of strong mainshocks, that requires a quasi-periodic behavior. This behavior is mainly determined by the tectonic loading on a faults' region (network of faults). On the other hand, the D-AS model is based on the triggering of mainshocks by their preshocks. That is, the procedure followed in the present work to estimate (predict) strong ensuing mainshocks is based on observed predictive properties of both physical processes which affect the earthquake generation, that is, tectonic loading and seismic triggering.

Estimation (prediction) of probably ensuing mainshocks in the broader Aegean is mainly based on the D-AS model, since this model allows the estimation of all three parameters of an ensuing mainshock (origin time, epicenter, magnitude), while the TIMAP model allows estimation of the epicenter and probability of occurrence of a strong (M≥6.0) mainshock during a certain time interval (e.g., Δt=10 years). Nevertheless, contribution of the TIMAP model is also

essential because this model is based on independent principles and data with respect to the D-AS model, while its failure ratio is small.

The application of the two models in a region requires an appropriate data set. The scaling coefficients of the basic formulas of the TIMAP model [Eqs. (1) and (2) in the present paper] have been calculated by a large sample of data (1811 interevent times) for mainshocks with a broad magnitude range ($6.0 \leq M \leq 8.5$), which occurred in several seismotectonic regimes (274 seismic regions). Therefore, these scaling coefficients are of global validity and hold for any large mainshock. The scaling constants Q and W (and the corresponding uncertainties σ_q and σ_w) must be reliably calculated by the available data for the study region. That is, the available data base for this region must include a large number of interevent times of strong mainshocks as is the case with the Aegean region studied in the present work.

The scaling coefficients and the constants of the basic formulas of the D-AS model (relations 11 to 15 in the present paper) are based on large samples of data concerning preshocks of mainshocks with a large magnitude range ($6.3 \leq M \leq 8.3$) occurring in several seismotectonic regimes. We have recently observed that the D-AS model also applies to giant mainshocks ($M \geq 8.5$, Sumatra 2004, South America 2010), with minor modifications. The database for a particular region is also of importance for application of the D-AS model in this region because this application requires reliable calculations of the strain rates (s_d and s_a) in the circular (seismogenic and critical) regions. For this purpose accurate and complete data are required. The condition for completeness is that required for the minimum magnitude, $M_{min,}$ of decelerating preshocks:

$$M_{\min} = 0.29M + 2.35 \tag{18}$$

where, M is the mainshock magnitude (Papazachos *et al*., 2006). Since for M=6.0, M_{min}=4.1, prediction of mainshocks with $M \geq 6.0$ by the D-AS model requires a database that must include information for shocks with $M \geq 4.1$.

It should be noted that the TIMAP model is based on inter-event times of mainshocks which occurred in a network of interacting seismic faults for which a large sample of observations is available for seismotectonically active areas like the Aegean. Previous relative works, however, deal mainly with inter-event times of mainshocks which occurred in the same seismic fault and for this reason the available samples of data are usually very limited even for very active faults. On the other hand, the D-AS model makes simultaneous use of accelerating and decelerating seismicity patterns which precede the same mainshock, while previous works usually concern only accelerating precursory seismicity or only precursory quiescence of seismicity.

In the present work an attempt is made to use inter-event times of mainshocks and properties of accelerating and decelerating preshocks to predict the same mainshock. The fact that application of both models in regions of the Aegean area gives similar results is encouraging for the continuation of this work by applying this procedure to other areas.

The algorithm developed for the D-AS model treats circular and elliptical seismogenic (decelerating preshocks) and critical (accelerating preshocks) regions. Application of this algorithm on already occurred preshock-mainshock sequences has shown that the results

obtained with circular and elliptical regions are very similar. This is probably due to the fact that such a region is defined by a network of seismic faults which forms an area which is not elongated as it occurs with a single seismic fault. Thus, circular regions are preferred because they are simple and require relatively short processing time.

The main result of the present work is that six strong ($M \geq 6.0$) shallow ($h \leq 100$ km) mainshocks are expected in the Aegean area during the next eight years (2010-2017). The parameters (epicenter coordinates, magnitude and origin time) and their uncertainties for these probably ensuing mainshocks came mainly from the application of the D-AS model. The generation of these six mainshocks during the next decade (2010-2019) and their location are supported by the TIMAP model.

Finally, it must be pointed out that the purpose of the present work is to improve knowledge on earthquake prediction. Thus, this paper is addressed to relevant scientists only.

Acknowledgements. The authors would like to thank both reviewers and the Associate Editor Lawrence Hutchings for their constructive criticism which helped to clarify certain aspects.

REFERENCES

Ben-Zion Y. and Lyakhovsky V.; 2002: *Accelerated seismic release and related aspects of seismicity patterns on earthquake faults.* Pure Appl. Geophys., **159**, 2385-2412.

Brehm D.J. and Braile L.W.; 1999: *Refinement of the modified Time-to-failure Method for intermediate-term earthquake prediction.* J. Seismology, **3**, 121-138.

Bufe C.G. and Varnes D.J.; 1993: *Predictive modeling of seismic cycle of the Great San Francisco Bay Region.* J. Geophys. Res., **98**, 9871-9883.

Fedotov S.A.; 1965: *Regularities of the distribution of strong earthquakes in Kamchatka, the Kurile Islands and Northeastern Japan.* Tr. Inst. Fiz. Zemli, Akad. Naua SSSR, **36**, 66-93, (in Russian).

Kagan Y.Y. and Jackson D.D.; 1991: *Long-term earthquake clustering.* Geophys. J. Int., **104**, 117-133.

Karakaisis G.F., Papazachos C.B. and Scordilis E.M.; 2010: *Seismic sources and main seismic faults in the Aegean and surrounding area.* Bull. Geol. Soc. Greece, **43**, 2026-2042.

Knopoff L., Levshina T., Keillis-Borok V.J. and Mattoni C.; 1996: *Increased long-rang intermediate-magnitude earthquake activity prior to strong earthquakes in California.* J. Geophys. Res., **101**, 5779-5796.

Mogi K.; 1969: *Some features of the recent seismic activity in and near Japan. II. Activity before and after great earthquakes.* Bull. Earthq. Res. Inst., Univ. Tokyo, **47,** 395-417.

Papazachos B.C. and Karakaisis G.F.; 2008: *Present space-time evolution of seismicity in the region of Greece.* Official Report to the Minister of Public Works of Greece, 30 June 2008, 7 pp.

Papazachos B.C. and Papaioannou Ch.A.; 1993: *Long term earthquake prediction in the Aegean area based on the time and magnitude predictable model.* Pure Appl. Geophys., **140**, 593-612.

Papazachos B.C. and Papazachou C.B.; 2003: *The earthquakes of Greece.* Ziti Publications, Thessaloniki, 273 pp.

Papazachos, B.C., Comninakis, P.E., Scordilis, E.M., Karakaisis, G.F. and Papazachos, C.B.; 2010a: *A catalogue of earthquakes in Mediterranean and surrounding area for the period 1901-2009.* Publ. Geoph. Laboratory, University of Thessaloniki. (http://geophysics.geo.auth.gr/ss/station_index_en.html).

Papazachos B.C., Karakaisis G.F., Papazachos C.B., Panagiotopoulos D.G. and Scordilis E.M.; 2009: *A forward test of the Decelerating-Accelerating Seismic Strain Model in the Mediterranean*. Boll. Geof. Teor. Appl., **50**, 235-254.

Papazachos B.C., Karakaisis G.F., Papazachos C.B. and Scordilis E.M.; 2007: *Evaluation of the results for an intermediate term prediction of the 8 January 2006 M_W=6.9 Cythera earthquake in southern Aegean.* Bull. Seism. Soc. Am., **97**, 347-352.

Papazachos B.C., Karakaisis G.F., Papazachos C.B., and Scordilis E.M.; 2010b: *Intermediate term earthquake*

prediction based on interevent times of mainshocks and on seismic triggering. Bull. Geol. Soc. Greece, **43**, 46-69.

Papazachos B.C., Papadimitriou E.E., Karakaisis G.F. and Panagiotopoulos D.G.; 1997: *Long-term earthquake prediction in the Circum-Pacific convergent belt.* Pure Appl. Geophys., **149**, 173-217.

Papazachos C.B., Karakaisis G.F., Savaidis A.S. and Papazachos B.C.; 2002: *Accelerating seismic crustal deformation in the southern Aegean area.* Bull. Seism. Soc. Am., **92**, 570-580.

Papazachos C.B., Karakaisis G.F., Scordilis E.M. and Papazachos B.C.; 2005a: *Global observational properties of the critical earthquake model.* Bull. Seism. Soc. Am., **95**, 1841-1855.

Papazachos C.B., Karakaisis G.F., Scordilis E.M. and Papazachos B.C.; 2006: *New observational information on the precursory accelerating and decelerating strain energy release.* Tectonophysics, **423**, 83-96.

Papazachos C.B., Scordilis E.M., Karakaisis G.F. and Papazachos B.C.; 2005b: *Decelerating preshock seismic deformation in fault regions during critical periods.* Bull. Geol. Soc. Greece, **36,** 1491-1498.

Robinson R.; 2000: A *test of the precursory accelerating moment release model on some recent New Zealand earthquakes.* Geoph. J. Int., **140**, 568-576.

Shimazaki K. and Nakata T.; 1980: *Time predictable recurrence model for large earthquakes.* Geophys. Res. Lett., **7**, 279-282.

Tocher D.; 1959: *Seismic history of the San Francisco bay region.* Calif. Div. Mines Spec. Rep., **57**, 39-48.

Tzanis A., Vallianatos F. and Makropoulos K.; 2000: *Seismic and electric precursors to the 17-1-1983, M7 Kefallinia earthquake, Greece: signatures of a SOC system*. Phys. Chem. Earth, **25**, 281-287.

Corresponding author: George Karakaisis
Department of Geophysics, School of Geology, Faculty of Science, Aristotle University,
GR54124, Thessaloniki, Greece,
Phone: +30 2310 998484; e-mail: karakais@geo.auth.gr